Int. J. Solids Structures Vol. 19, No. 10, pp. 885–894, 1983
Printed in Great Britain.

0020-7683/83 $3.00 + .00
Pergamon Press Ltd.

ELASTIC CONSTANTS OF FIBER-REINFORCED BORON-ALUMINUM: OBSERVATION AND THEORY

S. K. DATTA
Department of Mechanical Engineering and Cooperative Institute for Research in Environmental Sciences, University of Colorado, Boulder, CO 80309, U.S.A.

and

H. M. LEDBETTER
Fracture and Deformation Division, National Bureau of Standards, Boulder, CO 80303, U.S.A.

(*Received* 10 *May* 1982; *in revised form* 10 *February* 1983)

Abstract—Elastic constants, both the C_{ij}'s and S_{ij}'s, were measured and calculated for a laminated, uniaxially fiber-reinforced boron-aluminum composite. Three theoretical models were considered: square-array, hexagonal-array, and random-distribution. By combining several existing theoretical studies on randomly distributed fibers, we derived relationships for predicting the full set of elastic constants for this model. The random-distribution model agrees best with observation, especially for off-diagonal elastic constants. Considering all nine elastic constants, observation and theory differ on the average by 6%. These discrepancies arise from three sources: experimental error propagation, limited applicability of a transverse-isotropic model to a laminated composite, and elastic anisotropy of boron fibers.

1. INTRODUCTION

Fiber-reinforced composites have been studied extensively, both experimentally and theoretically. Recent reviews on this subject include that of experiment by Bert[1] and of theory by Sendeckyj[2].

Two types of fiber-reinforced composites occur in practice: continuous-fiber and short (chopped)-fiber. The former type has been studied more thoroughly and constitutes the object of this study.

Boron-fiber-reinforced aluminum, a so-called advanced-technology composite, was the particular material that was studied. The principal purpose of the study was to evaluate various models for predicting the composite's macroscopic elastic constants from those of its constituents. Three models, shown schematically in Fig. 1, were considered: square-array, hexagonal-array, and random-distribution. The composite's elastic constants were measured two ways: by ultrasonic-velocity measurements, which yield the C_{ij}'s, the elastic stiffnesses; and by standing-wave resonance, which yields the S_{ij}'s, the elastic compliances. These macroscopic elastic constants define for most cases the mechanical response of the composite to an applied force.

2. MATERIAL

The studied composite consisted of 0.14-mm-diameter boron fibers in an aluminum-alloy-6061 matrix. The alloy was in the F-tempered condition. The composite, containing 48% fibers by volume, was fabricated as a 10 × 10 × 1.1 cm plate containing about seventy plies. Figure 2 is a photomicrograph showing the distribution of fibers in the transverse

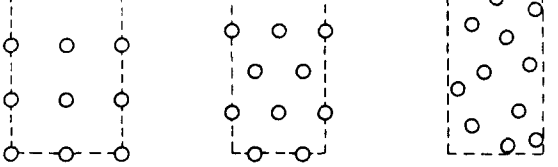

Fig. 1. Schematic diagram of fiber distribution for three models considered in this study: square-array, hexagonal-array, and random-distribution. Diagram shows intersection of fibers, parallel to x_3, with $x_1 - x_2$ plane.

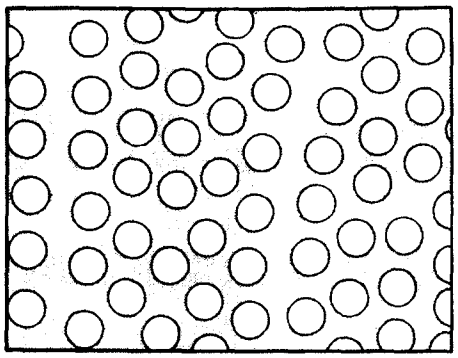

Fig. 2. Tracing of a photomicrograph showing distribution of 0.14-mm diameter boron fibers in an aluminum alloy matrix. Plane of photo is perpendicular to fibers, which are parallel to x_3 axis.

plane. This section usually showed cracks in most fibers. We guess that these defects arose mainly during specimen preparation. Two observations support this. First, more care in specimen preparation resulted in fewer cracks. Second, longitudinal sections showed dramatically fewer cracks; almost all of these ran across the fiber and not along it as would occur in fiber splitting. The relatively low internal friction of the composite also indicates a low crack density. Mass density, measured hydrostatically, was 2.534 g/cm^3.

Throughout this study we adopt the following coordinate system: x_3 is the fiber direction, x_1 is normal to the laminae plane, and x_2 is orthogonal to x_1 and x_3, (see Fig. 3). Thus, x_1 and x_2 are equivalent directions from the viewpoint of all three theoretical models considered here.

3. EXPERIMENTAL METHODS

Our experimental methods were chosen to provide the advantages of small specimens and low inaccuracy.

For brevity, experimental details are omitted here; they were described previously for both the ultrasonic-velocity method[3] and the resonance method[4].

Briefly, the ultrasonic-velocity method consisted of a pulse-echo technique using gold-plated piezoelectric crystals at frequencies near 10 MHz with specimen thickness varying from 0.2 to 1.0 cm. Except for an improved velocity-measurement system used in this study, it proceeded similarly to that described by Ledbetter and Read[5]. Reproducibility of measured sound velocities was typically within one to two percent.

The resonance method used a three-component (Marx) oscillator. Specimens were rod-shaped, about 0.4 cm in either circular or square cross section, and 4 to 10 cm long. Frequencies ranged from 30 to 50 kHz.

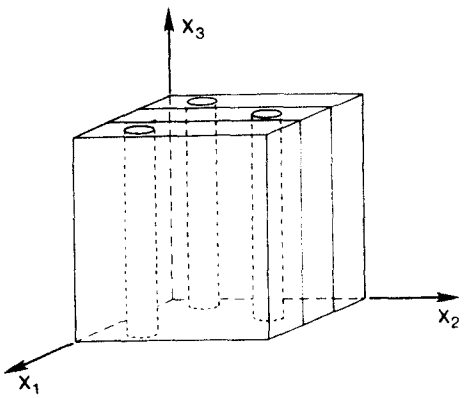

Fig. 3. Coordinate system adopted in this study. Fibers are parallel to x_3. Laminae lie in the $x_2 - x_3$ plane.

4. EXPERIMENTAL RESULTS

Results of the experimental studies are given in Tables 1 and 2 for the C_{ij}'s and the S_{ij}'s, respectively. The nine C_{ij}'s are based on a least-squares fit to eighteen separate wave-velocity propagation directions and polarizations. For details, see [5]. The five S_{ij}'s are based on extensional-mode and torsional-mode measurements on cylindrical specimens whose axes were in the $x_2 - x_3$ plane, as described by Read and Ledbetter[6]. The plate thickness of the studied material was too short to permit S_{ij} measurements along x_1. Thus, the measured S_{ij}'s are incomplete since they do not reflect the full orthotropic symmetry of the composite. However, as shown in Table 2, except for S_{66} and S_{12}, this incomplete set of S_{ij}'s differs only slightly from those derived from the observed C_{ij}'s, which do contain the full orthotropic symmetry.

Table 3 shows the elastic constants of the constituent materials; both being assumed isotropic. In this Table, ρ denotes mass density, E Young's modulus, μ shear modulus, B bulk modulus (reciprocal compressibility), k plane-strain bulk modulus for lateral dilatation without longitudinal extension, and λ the Lamé constant. For aluminum these parameters were determined ultrasonically, as described above, on a bulk specimen; their

Table 1. Observed and predicted C_{ij} elastic stiffnesses of a boron-aluminum unidirectionally fiber-reinforced composite, in units of 10^{11} N/m^2

ij	Observed	Square Model[a]	Hexagonal Model[b]	Random Model[c]	Full Random Model
11	1.852	1.856	1.872	1.790	1.790
22	1.797	1.856	1.872	1.790	1.790
33	2.450	2.480	2.551	---	2.560
44	0.566	0.451	0.561	0.559	0.559
55	0.569	0.451	0.561	0.559	0.559
66	0.526	---	0.606	0.523	0.523
12	0.779	---	0.661	---	0.745
13	0.606	---	0.578	---	0.583
23	0.604	---	0.578	---	0.583

[a]After Achenbach [9].
[b]After Hlavacek [10].
[c]After Bose and Mal [12].

Table 2. Observed and predicted S_{ij} elastic compliances of a boron-aluminum unidirectionally fiber-reinforced composite, in units of 10^{-11} m^2/N

ij	Observed[a]	From C_{ij}'s[b]	Predicted, Full Random Model
11	0.708	0.684	0.699
22	0.708	0.707	0.699
33	0.438	0.461	0.436
44	1.755	1.767	1.788
55	1.755	1.757	1.788
66	2.123	1.901	1.913
12	-0.353	-0.261	-0.258
13	-0.106	-0.105	-0.100
23	-0.106	-0.110	-0.100

[a]Assumed transverse-isotropic symmetry.
[b]Based on orthotropic symmetry.

Table 3. Properties of constituent materials

	ρ (g/cm^3)	E ($10^{11} N/m^2$)	μ ($10^{11} N/m^2$)	B ($10^{11} N/m^2$)	ν	k ($10^{11} N/m^2$)	λ ($10^{11} N/m^2$)
Boron	2.352	3.979	1.763	1.785	0.129	2.383	0.590
Aluminum alloy	2.702	0.715	0.267	0.751	0.341	0.840	0.573

uncertainty is less than 1%. Boron's elastic constants are less certain, a wide range of values being reported in the literature. The boron values in Table 3 arose from fitting a linear rule-of-mixtures to our observed S_{33} value combined with Gschneidner's[7] recommended values of boron's bulk modulus. These values agree within 0.5% with the Young's modulus and within 0.4% with the shear modulus reported for 0.203-mm-diameter fibers[8]. In Section 7, we discuss the assumption of isotropy for boron fibers.

5. THEORY

In Tables 1 and 2, the experimental results are compared with results of four theories: (1) that for a periodic square-lattice array of long, parallel, circular fibers derived by Achenbach[9] using a homogeneous continuum model that predicts three elastic constants; (2) similar to Achenbach's model, a hexagonal-array model derived by Hlavacek[10] that provides five elastic constants; (3) a random-distribution model due to Bose and Mal[11, 12], who derived expressions for three independent elastic constants; (4) a full-random-distribution model derived here by combining the results of [11, 12] with those of Hill[13]. This latter, present model predicts all five independent elastic constants of a matrix reinforced with long, parallel fibers distributed randomly in the transverse plane. The Achenbach, Hlavacek, and Bose-Mal models are described in the Appendix.

6. FULL RANDOM-DISTRIBUTION MODEL

In this section we show that combining the Bose–Mal relationships (see Appendix) with previously derived relationships for other elastic constants leads to a full set of five independent elastic constants for the random-distribution case. For this, a new notation[2] is useful, which will be described as it is introduced.

Hashin and Rosen[14] derived relationships for the effective moduli of a continuous-fiber-reinforced composite where the fibers are distributed randomly and homogeneously. Hashin[15] gave these relationships in essentially the form

$$k_T = k_m - \frac{c(k_f - k_m)(k_m + \mu_m)}{k_f + \mu_m - c(k_f - k_m)} \tag{1}$$

and

$$\mu_{LT} = \mu_m + \frac{2c(\mu_f - \mu_m)\mu_m}{\mu_f + \mu_m - c(\mu_f - \mu_m)}. \tag{2}$$

Here, k denotes the two-dimensional, plane-strain bulk modulus, which is $\lambda + \mu$ in an isotropic material. Subscript T denotes deformation in the $x_1 - x_2$ plane, perpendicular to the fibers. Subscript LT denotes shear deformation in any plane containing the x_3 axis, that is, the fiber axis. Equations (1) and (2) were also derived by Hill[13] for a single fiber placed concentrically in a cylindrical matrix. Hermans[16] obtained them also by considering Hill's assembly to be embedded in an unbounded solid having the effective elastic moduli of the composite. In this model, the fiber:matrix-cylinder radius ratio is $r_1/r_2 = c^{1/2}$.

Knowing k_T, one can derive the Young's modulus E_L (along x_3) and the Poisson's ratio $\nu_{LT} = -\epsilon_1/\epsilon_3$, where uniaxial stress is along x_3 and ϵ denotes strain. This is done by using the

relationship given by Hill[13]:

$$\frac{\frac{1}{k_T}-\frac{1}{k_f}}{\nu_{LT}-\nu_f}=\frac{\frac{1}{k_T}-\frac{1}{k_m}}{\nu_{LT}-\nu_m}=\frac{\frac{1}{k_f}-\frac{1}{k_m}}{\nu_f-\nu_m}=\frac{4\nu_{LT}-\nu_m-c(\nu_f-\nu_m)}{E_L-E_m-c(E_f-E_m)}. \tag{3}$$

Solving for E_L and ν_{LT}, using eqn (1), one finds

$$E_L=(1-c)E_m+cE_f+\frac{4c(1-c)(\nu_f-\nu_m)^2}{\frac{(1-c)}{k_f}+\frac{c}{k_m}+\frac{1}{\mu_m}} \tag{4}$$

and

$$\nu_{LT}=(1-c)\nu_m+c\nu_f+\frac{c(1-c)(\nu_f-\nu_m)\left(\frac{1}{k_m}-\frac{1}{k_f}\right)}{\frac{(1-c)}{k_f}+\frac{c}{k_m}+\frac{1}{\mu_m}}. \tag{5}$$

Of course, both of these relationships represent a simple, linear "rule of mixtures" plus a higher-order correction term. The advantages of eqns (1)–(2) are clear: they give simple, explicit relationships for four of the composite's elastic constants in terms of the isotropic elastic constants of the constituent materials, the fiber and the matrix. On the other hand, self-consistent approaches lead to implicit relationships.

Bose and Mal[11–12] also obtained eqns (1) and (2), but by a different approach: by considering the effective velocity for long-wavelength plane waves propagating perpendicular to the fibers, for both a longitudinal wave and for a shear wave polarized along x_3, the fiber axis. By a similar approach, examining a shear wave propagating and polarized in a plane transverse to the fibers, Bose and Mal[11] also derived an expression for the transverse shear modulus:

$$\mu_{TT}=\mu_m+\frac{2c(k_m+\mu_m)(\mu_f-\mu_m)}{k_m+\left(\frac{k_m}{\mu_m}+2\right)[c\mu_m+(1-c)\mu_f]}. \tag{6}$$

Previous studies[13, 14] did not obtain this explicit expression, but bounds instead. In fact, eqn (6) corresponds to the lower bound. Equations (1), (2), (4) and (5) are also identical to the lower-bound results. Thus, the "quasi-crystalline" approximation used by Bose and Mal to derive eqns (1), (2) and (5) leads to the lower-bound results, which these authors believe to be "nearer to the actual value if correlations are ignored." Equation (6) coincides also with Hermans'[16] result, which he points out "lies between the bounds derived by Hashin and Rosen." From the above relationships, one obtains for the boron–aluminum composite, using results in Table 3:

$$E_L=2.292\cdot 10^{11}\ \mathrm{N/m^2},$$
$$k_T=1.267\cdot 10^{11}\ \mathrm{N/m^2},$$
$$\mu_{LT}=0.559\cdot 10^{11}\ \mathrm{N/m^2},$$
$$\mu_{TT}=0.523\cdot 10^{11}\ \mathrm{N/m^2},$$
$$\nu_{LT}=0.230.$$

Since the composite behaves transversely isotropic with the unique symmetry axis along

x_3, the C_{ij} elastic-stiffness constants can be computed from

$$C_{11} = C_{22} = k_T + \mu_{TT}, \tag{7}$$

$$C_{33} = E_L + 2\nu_{LT}C_{13}, \tag{8}$$

$$C_{44} = C_{55} = \mu_{LT}, \tag{9}$$

$$C_{66} = \tfrac{1}{2}(C_{11} - C_{12}) = \mu_{TT}, \tag{10}$$

$$C_{12} = k_T - \mu_{TT}, \tag{11}$$

$$C_{13} = C_{23} = 2\nu_{LT}k_T. \tag{12}$$

These results are given in the final column of Table 1.

7. DISCUSSION

Here we consider principally the correspondence between observed C_{ij}'s and their counterparts predicted by three models: square-array, hexagonal-array, and random-distribution.

C_{33} is predicted reasonably well by all three models, although all are slightly high, perhaps reflecting the slight uncertainty in Young's modulus of the boron fibers.

C_{11} is predicted best by the lattice models, and C_{22} is predicted best by the random model. As shown in Fig. 2, this probably reflects the different imperfections in fiber distributions along the x_1 and x_2 directions.

C_{44} and C_{55}, which represent shears with the force parallel to the fibers, are not predicted accurately by the square-array model; but they are predicted well by both the hexagonal-array and the random models. Thus, these elastic constants permit one to distinguish fiber arrays that are transversely anisotropic (tetragonal, orthorhombic) from those that are transversely isotropic (hexagonal, random).

C_{66}, which represents shears with a force perpendicular to the fibers, is predicted well only by the random model. Since C_{66} represents also the velocity of a plane wave both propagated and polarized in the transverse plane, of all elastic constants it should be most sensitive to the fiber distribution. Thus, the different predictions for the hexagonal and random models, both of which are transversely isotropic, are not too surprising. Furthermore, Fig. 2 shows little evidence of either three-fold or six-fold symmetry around the fiber axis.

C_{12}, C_{13} and C_{23}, the so-called off-diagonal elastic constants, are predicted surprisingly well by the random model. Since these constants are always determined indirectly, whether experimentally or theoretically, one expects larger errors than for the diagonal elastic constants, the C_{ii}'s, discussed above. Absence of large discrepancies between observation and theory for these three elastic constants gives one simultaneous confidences in the experimental measurements and in the random-distribution model for this particular composite.

The bulk modulus,

$$B = \frac{1}{9}\sum_{i,j=1}^{3} C_{iijj}, \tag{13}$$

predicted by either the hexagonal model (1.103) or the full-random model (1.107) agrees well with observation (1.120). Since the bulk modulus includes six out of nine of the C_{ij}'s, barring fortuitous error cancellations, this observation-theory agreement within 1% also tends to establish the simultaneous credibility of both measurements and theory.

We remark that similar observations hold also for the S_{ij}'s, as shown in Table 2. However, these comparisons are less useful because only five S_{ij}'s were determined experimentally, compared with nine C_{ij}'s. Also, the experimental S_{66} is inconsistent with that predicted or that computed by inverting the C_{ij} matrix; this reflects also in the experimental S_{12} value and is believed to be an experimental artifact, related perhaps to

impure torsional modes about the x_2 axis. Except for this discrepancy, there are no differences between the 30-kHz S_{ij} results and the 10-MHz C_{ij} results; thus, measurable dispersion does not occur in this material in this frequency range. This absence of dispersion is especially interesting for the higher frequencies where the wavelength is not much larger than the fiber spacing or the fiber diameter.

In concluding we note that the observed C_{ij}'s can be used to derive the elastic constants of boron fibers. For this purpose, let k_T^f, μ_{TT}^f, be the transverse bulk and shear moduli of the fibers, respectively. Also, let the remaining constants be E_L^f, μ_{LT}^f, and ν_{LT}^f. Then one finds from eqns (1), (2) and (4)–(6) that

$$k_T^f = k_m + \frac{1}{\dfrac{c}{k_T - k_m} - \dfrac{1-c}{k_m - \mu_m}}, \tag{14}$$

$$\mu_{LT}^f = \mu_m + \frac{1}{\dfrac{c}{\mu_{LT} - \mu_m} - \dfrac{1-c}{2\mu_m}}, \tag{15}$$

$$E_L^f = \frac{1}{c}(E_L - (1-c)E_m) - \frac{4(1-c)(\nu_{LT}^f - \nu_m)^2}{\dfrac{1-c}{k_T^f} + \dfrac{c}{k_m} + \dfrac{1}{\mu_m}}, \tag{16}$$

$$\nu_{LT}^f = \frac{\left(\dfrac{1}{k_T^f} + \dfrac{1}{\mu_m}\right)(\nu_{LT} - (1-c)\nu_m) + c\nu_{LT}\left(\dfrac{1}{k_m} - \dfrac{1}{k_T^f}\right)}{c\left(\dfrac{1}{k_m} + \dfrac{1}{\mu_m}\right)}, \tag{17}$$

$$\mu_{TT}^f = \mu_m + \frac{1}{\dfrac{c}{\mu_{TT} - \mu_m} - \dfrac{(1-c)(k_m + 2\mu_m)}{2\mu_m(k_m + \mu_m)}}. \tag{18}$$

Then using the measured C_{ij}'s (Table 1) and eqns (7)–(12) the properties are found. These are used in eqns (14)–(18) to obtain the boron fiber properties:

$$\begin{gathered} k_T^f = 2.693 \times 10^{11}\ \text{N/m}^2,\ \mu_{LT}^f = 1.891 \times 10^{11}\ \text{N/m}^2 \\ \nu_{LT}^f = 0.130,\ E_L^f = 3.728 \times 10^{11}\ \text{N/m}^2,\ \mu_{TT}^f = 2.014 \times 10^{11}\ \text{N/m}^2. \end{gathered} \tag{19}$$

The transverse Young's modulus and Poisson's ratio of boron would then be

$$E_T^f = 4.515 \times 10^{11}\ \text{N/m}^2,\ \nu_T^f = 0.121.$$

Thus, boron fibers are slightly anisotropic. This anisotropy explains partly the differences in the observed and calculated C_{ij}'s.

8. CONCLUSIONS

A random-fiber-distribution model predicts successfully the elastic constants of a laminated, uniaxially fiber-reinforced boron-aluminum composite. For the six principal C_{ij} ($C_{ij} = C_{ii}$, $i = 1$–6), theory and observation differ on average by 2%. The C_{66} elastic shear stiffness provides the most discriminating test of various fiber-distribution models. Conversely, the observed C_{66} provides the best gage of fiber distribution (square, hexagonal, random). Reverse application of theory (macroscopic to constituent) indicates that the boron fibers are slightly anisotropic.

Acknowledgments—This study was supported by the NBS Office of Nondestructive Evaluation. Most of the sound-velocity measurements were made by M. W. Austin. A first draft of the manuscript was completed while

H. M. Ledbetter visited the Institute for Theoretical and Applied Physics at the University of Stuttgart. J. Dahnke contributed valuably to constructing the manuscript.

REFERENCES

1. C. W. Bert, Experimental characterization of composites. In *Composite Materials*, Vol. 8, pp. 73–133. Academic Press, New York (1975).
2. G. P. Sendeckyj, Elastic behavior of composites. In *Composite Materials*, Vol. 2, pp. 45–83. Academic Press, New York (1974).
3. H. M. Ledbetter, Dynamic elastic modulus and internal fraction in fibrous composites. In *Nonmetallic Materials and Composites at Low Temperatures*, pp. 267–281. Plenum Press, New York (1979).
4. H. M. Ledbetter, N. V. Frederick and M. W. Austin, Elastic-constant variability in stainless-steel 304. *J. Appl. Phys.* **51**, 305–309 (1980).
5. H. M. Ledbetter and D. T. Read, Orthorhombic elastic constants of an NbTi/Cu composite superconductor. *J. Appl. Phys.* **48**, 1874–1879 (1977).
6. D. T. Read and H. M. Ledbetter, Elastic constants of a boron–aluminum composite at low temperatures. *J. Appl. Phys.* **48**, 2827–2831 (1977).
7. K. A. Gschneidner, Physical properties and interrelationships of metallic and semimetallic elements. In *Solid State Physics*, Vol. 16, pp. 275–426. Academic Press, New York (1964).
8. J. A. DiCarlo, Mechanical and physical properties of modern boron fibers. *NASA Tm*-73882 (1978).
9. J. D. Achenbach, Generalized continuum theories for directionally reinforced solids. *Arch. Mech.* **28**, 257–278 (1976).
10. M. Hlavacek, A continuum theory of fibre-reinforced composites. *Int. J. Solids Structures* **11**, 199–211 (1975).
11. S. K. Bose and A. K. Mal, Longitudinal shear waves in a fiber-reinforced composite. *Int. J. Solids Structures* **9**, 1075–1085 (1973).
12. S. K. Bose and A. K. Mal, Elastic waves in a fiber-reinforced composite. *J. Mech. Phys. Solids* **22**, 217–229 (1974).
13. R. Hill, Theory of mechanical properties of fibre-strengthened materials: I. Elastic behaviour. *J. Mech. Phys. Solids* **12**, 199–212 (1964).
14. Z. Hashin and B. W. Rosen, The elastic moduli of fiber-reinforced materials. *J. Appl. Mech.* **31**, 223–232 (1964).
15. Z. Hashin, Theory of composite materials. In *Mechanics of Composite Materials*, pp. 201–242. Academic Press, New York (1970).
16. J. J. Hermans, The elastic properties of fiber reinforced materials when the fibers are aligned. *Proc. K. Ned. Akad. Wet.* **B70**, 1–9 (1967).

APPENDIX

Summary of other theoretical models

(i) *Square-array model.* For a periodic square lattice array of long, parallel, circular fibers, using a homogeneous continuum model, Achenbach[9] derived three relationships for plane, harmonic wave-propagation velocities expressed as ρv^2. Simplified and modified for present purposes, and with obvious notational correspondences, these are as follows.

For a longitudinal wave propagating along x_3, parallel to the fibers:

$$\rho v^2 = C_{33} = a_1 - \frac{a_3^2}{a_2}, \tag{A1}$$

where

$$a_1 = c(\lambda_f + 2\mu_f) + (1-c)(\lambda_m + 2\mu_m),$$
$$a_2 = 4c(\lambda_f + \mu_f),$$
$$a_3 = 2c\lambda_f.$$

For a longitudinal wave propagating along x_1, perpendicular to the fibers:

$$\rho v^2 = C_{11} = C_{22} = \mu_m/4M, \tag{A2}$$

where

$$M = \frac{c[cD - (1-c)B] + (1-c)[(1-c)A - cB]}{4(AD - B^2)},$$

$$A = a_{22_f} - \frac{(1-c)^2}{c} a_{23_f}^2 \frac{d}{q}\frac{1}{\mu_m},$$

$$B = (1-c)a_{23_f}a_{23_m}\frac{d}{q}\frac{1}{\mu_m},$$

$$D = a_{22_m} - ca_{23_m}^2\frac{d}{q}\frac{1}{\mu_m},$$

$$\frac{d}{q} = \frac{c}{(1-c)^2 a_{22_f} + c^2 a_{22_m}},$$

$$a_{22_f} = c(\lambda_f + 2\mu_f),$$

$$a_{23_f} = c\lambda_f,$$

$$a_{22_m} = (1-c)(\lambda_m + 2\mu_m) + \frac{2}{\pi(4-\pi)} c\mu_m + \frac{(\pi)^{1/2}}{c} - 2\frac{c}{\pi}\mu_m,$$

$$a_{23_m} = (1-c)\lambda_m + \frac{4}{\pi(4-\pi)} c\mu_m.$$

For a transverse wave propagating along x_3, parallel to he fibers, and polarized along x_1, perpendicular to the fibers:

$$\rho v^2 = C_{55} = C_{44} = a_1 - \frac{a_2^2}{a_3}, \tag{A3}$$

where

$$a_1 = c\mu_f + (1-c)\mu_m,$$
$$a_2 = c(\mu_f - \mu_m),$$
$$a_3 = c\mu_f + \frac{c^2}{1-c}\mu_m.$$

The Lamé constants, λ and μ, of the fiber and matrix are denoted by subscripts f and m; c denotes the volume fraction of fibers, 0.48 for the present case, and equals $\pi r^2/d^2$, where r denotes fiber radius and d distance between fiber centers in a square lattice. Clearly, $r/d = 0.3909$, or $d/r = 2.5583$. The constants a_1, a_2, a_3, etc., arise from the strain-energy density in Achenbach's derivation.

(ii) *Hexagonal-array model.* In calculations similar to Achenbach's, the five independent elastic constants consisting of parallel fibers arranged hexagonally were derived by Hlavacek[10]. His relationships, rearranged for present purposes, are as follows.

For a longitudinal wave propagating along x_1, perpndicular to the fibers:

$$\rho v^2 = C_{11} = C_{22} = a_1 - \frac{2a_7 a_8 a_{23} - a_{22}(a_7^2 + a_8^2)}{a_{22}^2 - a_{23}^2}, \tag{A4}$$

where

$$a_1 = (3V+1)\lambda_m + (7V+2)\mu_m,$$
$$a_7 = -V(3\lambda_m + 7\mu_m),$$
$$a_8 = -V(\lambda_m + \mu_m),$$
$$a_{22} = -c(\lambda_f + 2\mu_f) - (3V - c)\lambda_m - (7V - 2c)\mu_m,$$
$$a_{23} = -c\lambda_f - (V-c)\lambda_m - V\mu_m,$$
$$V = \frac{-c}{8(1-c^{1/2})^2}\ln c.$$

For a longitudinal wave propagating along x_3, parallel to the fibers:

$$\rho v^2 = C_{33} = a_{15} + \frac{2a_{18}^2}{a_{22} + a_{23}}, \tag{A5}$$

where

$$a_{15} = c(\lambda_f + 2\mu_f) + (1-c)(\lambda_m + 2\mu_m)$$

and

$$a_{18} = c(\lambda_f - \lambda_m).$$

For a transverse wave propagating along x_1, perpendicular to the fibers, and polarized along x_3, parallel to the fibers:

$$\rho v^2 = C_{44} = C_{55} = a_3 + \frac{a_{10}^2}{a_{28}}, \tag{A6}$$

where

$$a_3 = c\mu_f + (1-c)\mu_m,$$
$$a_{10} = c(\mu_f - \mu_m),$$
$$a_{28} = -c\mu_f - (4V - c)\mu_m.$$

For a transverse wave propagating along x_1, perpendicular to the fibers, and polarized along x_2, perpendicular to the fibers:

$$\rho v^2 = C_{66} = -a_2 + \frac{2a_8a_9a_{26} - a_{25}(a_8^2 + a_9^2)}{a_{25}^2 - a_{26}^2}, \tag{A7}$$

where

$$a_2 = V\lambda_m + (5V + 1)\nu_m,$$
$$a_9 = -V(\lambda_m + 5\mu_m),$$
$$a_{25} = -c\mu_f - V\lambda_m - (5V - c)\mu_m,$$
$$a_{26} = -c\mu_f - V\lambda_m - (V - c)\mu_m.$$

For the fifth independent elastic constant, Hlavacek derived an expression for $C_{13} + C_{44}$, which is related to the propagation of a transverse wave:

$$C_{13} = \frac{a_5a_{28} + a_{10}a_{19}}{a_{28}} + \frac{a_{18}(a_7 + a_8)}{(a_{22} + a_{23})}, \tag{A8}$$

where

$$a_5 = \lambda_m + \mu_m$$

and

$$a_{19} = -4V\mu_m.$$

In Hlavacek's model, the fiber volume concentration, c, equals r_1/r_2, the ratio of the fiber radius to that of the circle radius that equals the hexagonal "unit-cell" area. Constants, a_1, a_2, a_3, etc., arise from Hlavacek's equations of motion.

(iii) *Random-distribution model.* Considering the propagation of time-harmonic elastic waves in a composite of circular-cross-section, parallel fibers distributed randomly in a matrix, Bose and Mal[11, 12] derived expressions for three elastic moduli.

For a longitudinal wave propagating along x_1, perpendicular to the fibers:

$$\rho v^2 = C_{11} = C_{22} = \frac{[1 - c(1 - c^2)P_2 - 2c^2P_0P_2](\lambda_m + 2\mu_m)}{(1 + cP_0)[1 + c(1 + c^2)P_2]}, \tag{A9}$$

where

$$P_0 = \frac{\lambda_m + \mu_m - \lambda_f - \mu_f}{\lambda_f + \mu_f + \mu_m}$$

and

$$P_2 = \frac{\mu_m(\mu_m - \mu_f)}{\mu_f(\lambda_m + 3\mu_m) + \mu_m(\lambda_m + \mu_m)}.$$

For a transverse wave propagating along x_1, perpendicular to the fibers, and polarized along x_3, parallel to the fibers:

$$\rho v^2 = C_{11} = C_{22} = \left[1 + \frac{2c(\mu_f - \mu_m)}{\mu_f + \mu_m - c(\mu_f - \mu_m)}\right]\mu_m. \tag{A10}$$

For a transverse wave propagating along x_2, perpendicular to the fibers, and polarized along x_1, perpendicular to the fibers:

$$\rho v^2 = C_{66} = \tfrac{1}{2}(C_{11} - C_{12}) = \left[1 + \frac{2c(\lambda_m + 2\mu_m)(\mu_f - \mu_m)}{2\mu_m(\lambda_m + 2\mu_m) + (1 - c)(\lambda_m + 3\mu_m)(\mu_f - \mu_m)}\right]\mu_m. \tag{A11}$$